



# Efficient synthesis of ethylene glycol from cellulose over Ni–WO<sub>3</sub>/SBA-15 catalysts



Yueling Cao<sup>a,b</sup>, Junwei Wang<sup>a,\*</sup>, Maoqing Kang<sup>a</sup>, Yulei Zhu<sup>a</sup>

<sup>a</sup> Institute of Coal Chemistry, Chinese Academy of Sciences, Taiyuan 030001, PR China

<sup>b</sup> University of Chinese Academy of Sciences, Beijing 100049, PR China

## ARTICLE INFO

### Article history:

Received 9 July 2013

Received in revised form 5 October 2013

Accepted 7 October 2013

Available online xxx

### Keywords:

Cellulose

Ethylene glycol

Hydrogenolysis

Ni–WO<sub>3</sub>/SBA-15

## ABSTRACT

Ni–WO<sub>3</sub>/SBA-15 catalysts were prepared by an impregnation way and applied to the hydrogenolysis of cellulose in aqueous solution. The effect of nickel and WO<sub>3</sub> loading, catalysts reduction temperature and time on cellulose conversion were investigated. Up to 70.7% ethylene glycol yield was obtained over 3%Ni–15%WO<sub>3</sub>/SBA-15 catalysts. Several physicochemical methods such as XRD, Raman spectroscopy, NH<sub>3</sub>-TPD, H<sub>2</sub>-TPR and XPS were used to determine the character of catalysts. Based on these studies, it was found that there was a strong electronic interaction between NiO and WO<sub>3</sub>, which not only promoted the reduction of WO<sub>3</sub>, but restrained the reduction of NiO. Together with the experimental results, it can be concluded that the WO<sub>3-x</sub>, which may be the active species for the selective cleavage of C–C bond, was formed after catalysts pretreatment process. Additionally, a possible catalytic mechanism was proposed.

© 2013 Elsevier B.V. All rights reserved.

## 1. Introduction

Biomass is a kind of renewable energy resource generated by photosynthesis and comes from a variety of sources. Cellulose is the largest component of biomass and non-edible [1]. So the utilization of cellulose as feedstock for chemical and energy industries has attracted considerable attention. Unfortunately, cellulose is resistant to its depolymerization under mild conditions in conventional solvents since the abundant intra- and inter-molecular hydrogen bonds protect the β-1,4-glycosidic bonds from being attacked by foreign molecules [2].

Recently, series of heterogeneous catalysts were successfully applied to facilitate cellulose depolymerization in hydrothermal conditions. For the one-step conversion of cellulose, there are two types of desired products, sugar alcohols and ethylene glycol (EG). They are widely used in chemical industries, such as polymers, food, coating, detergent, and pharmaceutical industries. Since Fukuoka and Dhepe [3] presented the conversion of cellulose into sugar alcohols (sorbitol and mannitol) over a Pt/γ-Al<sub>2</sub>O<sub>3</sub>, many groups have also reported the conversion of cellulose into sugar alcohols, such as Ru/C, Ru/CNT, Ni/carbon nanofibers and Ni<sub>2</sub>P/activated carbon [4–7]. To boost the hydrolysis of cellulose, solid or liquid acids were introduced into the reaction, such as heteropolyacids

combined with Ru/C, mineral acid combined with Ru/C and mineral acid combined with Ru/USY [8–11]. Meanwhile, the selective conversion of cellulose to EG was noticed and widely studied over various catalyst systems. Among these catalysts, tungsten-based ones, especially when combining with the hydrogenation component, were proved to be a better choice due to the high catalytic activity and selectivity. For example, Ni–W<sub>2</sub>C/activated carbon, Ni–W/SBA-15, Ni–WxC/CMK-3, Ni–W/SiO<sub>2</sub>–Al<sub>2</sub>O<sub>3</sub>, Ru/C combined with WO<sub>3</sub> and Ru/C combined with H<sub>2</sub>WO<sub>4</sub> [12–17].

Apparently, various tungsten-based catalysts are effective in transforming cellulose into EG. However, few reports focus on the Ni–WO<sub>3</sub> system, or discuss the real active species for the high EG selectivity in detail. In this paper, a series of Ni–WO<sub>3</sub>/SBA-15 catalysts were prepared and applied to the direct conversion of cellulose under hydrogen pressure in aqueous solution. The effect of Ni, WO<sub>3</sub> loading and catalysts pretreatment conditions on cellulose conversion were investigated. The interaction between NiO and WO<sub>3</sub> was discussed based on the characterization results of XRD, Raman spectroscopy, NH<sub>3</sub>-TPR, H<sub>2</sub>-TPR and XPS. Moreover, a possible reaction mechanism of the selective catalytic conversion cellulose was proposed.

## 2. Experimental

### 2.1. Materials

Cellulose (Aladdin Chemistry Co. Ltd, microcrystalline), tungstophosphoric acid hydrate [H<sub>3</sub>O<sub>40</sub>PW<sub>12</sub>·xH<sub>2</sub>O] (Sinopharm

\* Corresponding author at: Institute of Coal Chemistry, Chinese Academy of Sciences, Taiyuan 030001, PR China. Tel.: +86 351 4069680; fax: +86 351 4069680.

E-mail address: [wangjw@sxicc.ac.cn](mailto:wangjw@sxicc.ac.cn) (J. Wang).

Chemical Reagent Co. Ltd., analytic grade), nickel nitrate hexahydrate [ $\text{Ni}(\text{NO}_3)_2 \cdot 6\text{H}_2\text{O}$ ] (Sinopharm Chemical Reagent Co. Ltd., analytic grade), and SBA-15 zeolite (Shanghai Novel Chemical Technology Co., Ltd.)

## 2.2. Preparation of catalysts

All catalysts were prepared by a conventional incipient impregnation method. Firstly, the support, SBA-15, was impregnated with a aqueous solution containing tungstophosphoric acid hydrate [ $\text{H}_3\text{O}_{40}\text{PW}_{12} \cdot x\text{H}_2\text{O}$ ] and nickel nitrate hexahydrate [ $\text{Ni}(\text{NO}_3)_2 \cdot 6\text{H}_2\text{O}$ ]. The impregnation volume of metal solution was calculated using the measured incipient wetness of the support. The impregnated catalysts were dried at  $100^\circ\text{C}$  for 12 h and then calcined at  $500^\circ\text{C}$  for 3 h. The monometallic catalysts were prepared by impregnation with the corresponding metal precursors mentioned above. Before the reaction, all of the catalysts were reduced in a hydrogen flow. The catalysts are labeled as  $x\%$  Ni/support,  $y\%$   $\text{WO}_3$ /support or  $x\%$  Ni– $y\%$   $\text{WO}_3$ /support, in which  $x$  and  $y$  stand for the nominal weight loading of Ni and  $\text{WO}_3$ , respectively.

## 2.3. Characterization

The bulk crystalline structures of the catalysts were determined using the X-ray diffraction (XRD) technique. The XRD patterns were obtained with a D8 ADVANCE using  $\text{Cu K}\alpha$  radiation.

Raman spectra were collected in ambient conditions with a resolution of  $1.5\text{ cm}^{-1}$  on Renishaw 1000 micro-Raman spectroscopy using a 632.8 nm He–Ne laser. For the 3%Ni–15%  $\text{WO}_3$ /SBA-15 catalyst (reduced), it was reduced at  $500^\circ\text{C}$  for 1 h. After that, its Raman spectrum was obtained without special protection.

The temperature-programmed desorption of ammonia ( $\text{NH}_3$ -TPD) was conducted in an AutoChem 2910 unit (Micromeritics)

equipped with a thermal conductivity detector (TCD). Quartz U-tube reactors were generally loaded with 0.10 g of the sample with a size in the range of 60–80 mesh, and the unreduced catalysts were pretreated in He at  $500^\circ\text{C}$  for 1 h, then cooled to  $120^\circ\text{C}$ . The charged sample was treated in 10 vol.%  $\text{NH}_3$ /He at  $120^\circ\text{C}$  for 10 min, and then the catalyst was flushed with He for 1 h. The  $\text{NH}_3$ -TPD was performed using 30 ml/min of He by heating the sample from  $120^\circ\text{C}$  to  $550^\circ\text{C}$  at a heating rate of  $10^\circ\text{C}/\text{min}$  while monitoring the TCD signals.

TPR experiments were carried out in a ChemBet 3000 equipped with a thermal conductivity detector (TCD). In the TPR experiments, the samples were pretreated in situ at  $450^\circ\text{C}$  for 1 h under  $\text{N}_2$  flow and cooled to  $40^\circ\text{C}$  in an  $\text{N}_2$  stream. The reduction step was performed with an 10 vol.%  $\text{H}_2/\text{N}_2$  mixture, with a heating rate of  $10^\circ\text{C}/\text{min}$ , up to  $700^\circ\text{C}$ . To investigate the effect of catalysts reduction temperature, all the 3%Ni–15%  $\text{WO}_3$ /SBA-15 catalysts were pretreated in situ at different temperature (from  $350^\circ\text{C}$  to  $600^\circ\text{C}$ ) for 1 h with 10 vol.%  $\text{H}_2/\text{N}_2$  flow. In the experiments of studying the impact of catalysts reduction time, all the 3%Ni–15%  $\text{WO}_3$ /SBA-15 catalysts were pretreated in situ at  $500^\circ\text{C}$  for different reduction time (from 10 min to 90 min) with 10 vol.%  $\text{H}_2/\text{N}_2$  flow.

The XPS spectra were obtained by using Al  $\text{K}\alpha$  radiation (1486.6 eV) through an AXIS ULTRA DLD system at a base pressure of  $10^{-6}$  Pa equipped an electronic neutralization gun to eliminate the charge effect on the sample surface. All the binding energies were calibrated by using contaminant carbon (C 1S = 284.6 eV) as a reference. For the 3%Ni–15%  $\text{WO}_3$ /SBA-15 catalyst (reduced), it was reduced at  $500^\circ\text{C}$  for 1 h. Without special protection, it was

quickly transferred to the analysis chamber of the spectrometer with a controlled-atmosphere transporter.

## 2.4. Catalytic experiments

All catalytic experiments were carried out in a 100 mL stainless-steel autoclave. Firstly, 1.0 g cellulose, 40 g deionized water, and 0.25 g catalysts were charged into the autoclave simultaneously, then the reactor was purged with hydrogen to remove air. Secondly, the reactor was filled with 6 MPa hydrogen pressure at room temperature and finally heated to  $230^\circ\text{C}$  with a strong stirring. After the reaction, the autoclave was cooled to room temperature with water, and the solid residues were filtered from the liquid products.

## 2.5. Product analysis

Products were quantified by both gas chromatography (GC) and high performance liquid chromatography (HPLC). The polyols, including EG, 1,2 – propylene glycol (1,2-PG), 1,2 – butanediol (1,2-BG), 1,2 – hexylene glycol (1,2-HG) and glycerol, were analyzed by a Shimadzu GC-2014, equipped with a flame ionization detector (FID) and HW workstation. The samples were injected (split ratio: 50) into a CBP20 (polar) column of  $25\text{ m} \times 0.22\text{ mm}$  and  $0.25\text{ }\mu\text{m}$  film thickness. The temperature program was as follows: holding at  $75^\circ\text{C}$  for 5.0 min, then increasing from  $75^\circ\text{C}$  to  $240^\circ\text{C}$  at a rate of  $30^\circ\text{C}/\text{min}$ , finally holding at  $240^\circ\text{C}$  for 20 min. Injector and detector temperatures were set as  $250^\circ\text{C}$  and  $280^\circ\text{C}$ , respectively. The hexitols were determined by HPLC with Ca-NP capillary chromatography column and evaporative light scattering detector. The detection was performed under the conditions: detection temperature of  $70^\circ\text{C}$ , column temperature of  $80^\circ\text{C}$ , mobile phase of deionized water with a flow rate of 0.6 ml/min.

The cellulose conversion and the polyol yield were calculated based on the following formulas [12]:

$$\text{Conversion}(\%) = \frac{\text{weight of cellulose before the reaction} - \text{weight of cellulose after the reaction}}{\text{weight of cellulose of before the reaction}} \times 100\%$$

$$\text{Yield}(\%) = \frac{\text{weight of the products determined}}{\text{weight of cellulose charged into the reactor}} \times 100\%$$

## 3. Results and discussion

### 3.1. Catalysts characterization

In order to characterize the bulk crystalline structures of various catalysts, the XRD analysis was conducted. Fig. 1 shows the XRD patterns of different samples. According to the XRD patterns of 15%Ni– $\text{WO}_3$ /SBA-15 with different  $\text{WO}_3$  loading (Fig. 1A), all catalysts showed peaks at  $2\theta$  ( $^\circ$ ) = 44.3, 51.5 and 75.8 due to the formation of metal Ni crystallites (ICDD: 65-0380). In contrast, when  $\text{WO}_3$  loading was 5% and 10%, respectively, even up to 15%, there were no manifest  $\text{WO}_2$  crystallite peaks. But further increasing  $\text{WO}_3$  loading to 20%, two crystalline  $\text{WO}_2$  peaks appeared at  $37.0^\circ$  and  $53.2^\circ$  (ICDD: 32-1393), indicating the congregation of tungsten oxide with the increase of  $\text{WO}_3$  loading. More importantly, it can prove that the existence of NiO promote the reduction of  $\text{WO}_3$ , which is in line with the  $\text{H}_2$ -TPR results as discussed below.

Considering the higher Ni loadings covering the active sites of  $\text{WO}_3$ , which would weaken the ability of catalysts for the selective cleavage of C–C bond, the catalysts with 15%  $\text{WO}_3$  and various Ni loading were prepared. Fig. 1B shows the XRD patterns of these catalysts. For the 1%Ni–15% $\text{WO}_3$ /SBA-15 sample, the reflections appeared at  $25.9^\circ$ ,  $37.0^\circ$  and  $53.2^\circ$  corresponding to the crystalline  $\text{WO}_2$ . The congregation of  $\text{WO}_2$  may be resulted from the

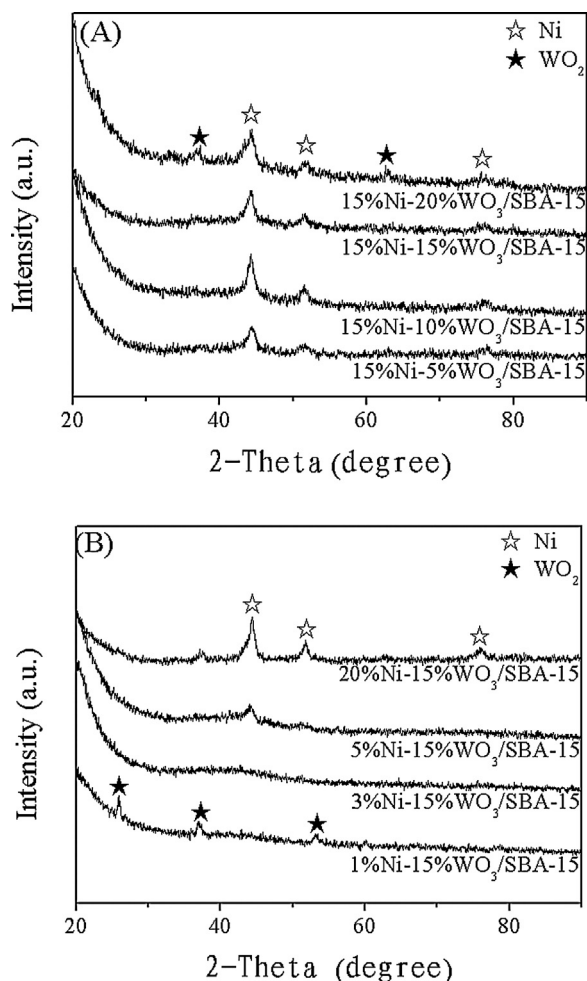


**Fig. 1.** Wide-angle XRD patterns of various catalysts. (a) 15%Ni-WO<sub>3</sub>/SBA-15 with different WO<sub>3</sub> loading. (b) Ni-15%WO<sub>3</sub>/SBA-15 with different Ni loading.

insufficient interaction between the NiO and WO<sub>3</sub> since the low Ni loading. When the Ni loading was 3% (molar ratio of Ni to W close to 1), there was a strong interaction between them resulting in the disappearing of crystalline WO<sub>2</sub> peaks. This result is consistent with Raman result that the crystalline WO<sub>3</sub> peaks disappeared due to the introduction of NiO. When the Ni loading was up to 20%, the appearing again of one weak peak at 37.0° indicated the presence of crystalline WO<sub>2</sub>, which might be due to the total loading (35%) was too high. From the discussion above, we can conclude that the low valence state tungsten was formed after the pretreatment process of catalysts.

Raman measurements were performed since this technology is a very powerful tool for phase analysis of tungsten oxides. Fig. 2 shows the Raman spectra of various samples. For the 3%Ni/SBA-15 sample, there was no peak appeared, while a significant difference was observed at sample of 15%WO<sub>3</sub>/SBA-15. The two Raman peaks at 715 and 807 cm<sup>-1</sup> were assigned to the O–W–O modes and the peaks at 270 and 330 cm<sup>-1</sup> were due to the bending vibration δ(O–W–O), which are the characteristic of monoclinic WO<sub>3</sub> [18]. Notably, the Raman spectrum of 15%WO<sub>3</sub>/SBA-15 sample showed no peak at 952 cm<sup>-1</sup>, which associated with the vibration of the terminal W=O bonds. These results might suggest that the tungsten oxide in 15%WO<sub>3</sub>/SBA-15 sample was formed by O–W–O micro-crystalline clusters connected to each other by W–O–W, with little terminal W=O bonds at the surface of the clusters. Conversely, the Raman spectrum of 3%Ni–15%WO<sub>3</sub>/SBA-15 showed only one peak at 952 cm<sup>-1</sup>; however the vibration range between 200 and

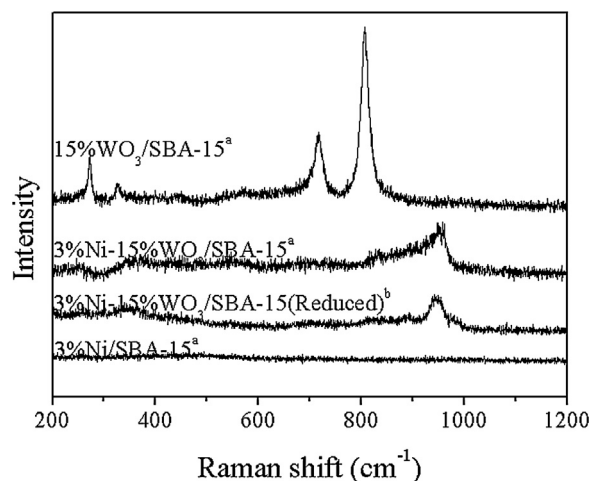


**Fig. 2.** Raman spectra of different catalysts. (a) These samples were unreduced. (b) 3%Ni–15%WO<sub>3</sub>/SBA-15 (reduced) was pretreated at 500 °C for 1 h in H<sub>2</sub> flow.

400 cm<sup>-1</sup> and the high-frequency area between 600 and 900 cm<sup>-1</sup> were disappeared. On the other hand, it was reported [19] that the ratio of the integrated Raman scattering intensities of the W=O band to that of the O–W–O band in the region of 600–900 cm<sup>-1</sup> could be used to measure the relative cluster size of tungsten oxide. The quantity of W=O terminal bonds around the cluster is inversely proportional to the cluster size. Based on above discussion, it can be concluded that surface polytungstate species may transform into monotungstate since the induction of NiO destroyed the crystal structure of WO<sub>3</sub>. On the other hand, it might also result in an interaction between NiO and WO<sub>3</sub> as mentioned above. For the Raman spectrum of reduced 3%Ni–15%WO<sub>3</sub>/SBA-15 sample, its Raman spectrum was similar with the unreduced 3%Ni–15%WO<sub>3</sub>/SBA-15 sample's, indicating there was still a strong interaction between metal Ni and tungsten oxide since the process of reduction did not break the structure of small tungsten oxide clusters.

NH<sub>3</sub>-TPD was carried out to study the surface acidity of different catalysts. The results are shown in Fig. 3. It can be found that the 3%Ni/SBA-15 catalyst almost had no acidity, and the very weak peak might result from the signal fluctuations. On the contrary, a broad peak of ammonia desorption at about 200 °C was detected on the surface of 15% WO<sub>3</sub>/SBA-15 catalyst, which indicated the presence of acidic sites on the surface as previous report [20]. Notably, compared with 15% WO<sub>3</sub>/SBA-15, the ammonia desorption peak

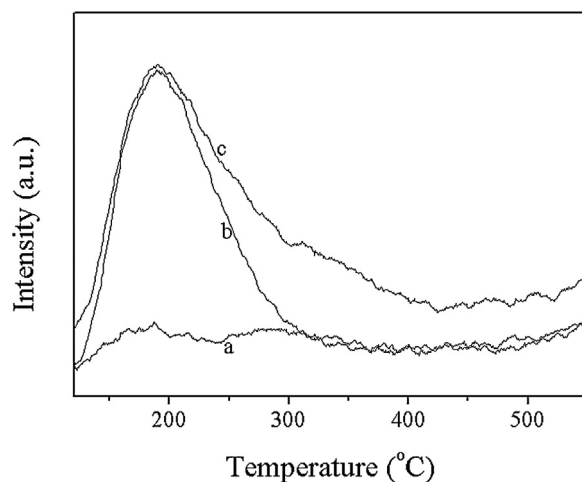


**Fig. 3.** NH<sub>3</sub>-TPD patterns of different catalysts (all of them were unreduced). (a) 3%Ni/SBA-15 (b) 15%WO<sub>3</sub>/SBA-15 (c) 3%Ni–15%WO<sub>3</sub>/SBA-15.

of 3%Ni–15% WO<sub>3</sub>/SBA-15 shifted to higher temperature, demonstrating that the introduction of NiO may contribute to increase the acid strength of WO<sub>3</sub>.

More information through hydrogen consumption and shifting of the reduction temperature could be obtained by TPR to elucidate the interactions between metal and metal. The TPR curves of various catalysts are presented in Fig. 4. As expected, the H<sub>2</sub>-TPR pattern of mechanical mixture of 3%Ni/SBA-15 and 15% WO<sub>3</sub>/SBA-15 was almost the same as their respective H<sub>2</sub>-TPR patterns since there was no interaction between NiO and WO<sub>3</sub>. The 3%Ni–15%WO<sub>3</sub>/SBA-15 catalyst prepared by co-impregnation showed reduction behavior significantly different from the observed for the mechanical mixture one. For the 3%Ni–15%WO<sub>3</sub>/SBA-15 catalysts, the initial reduction temperature of NiO (350 °C) was higher than that of 3%Ni/SBA-15 (300 °C). It is interesting to notice that the H<sub>2</sub> consumption area of 3%Ni–15%WO<sub>3</sub>/SBA-15 between 300 °C and 500 °C was far more than the sum area of 3%Ni/SBA-15 and 15% WO<sub>3</sub>/SBA-15. In addition, it is known that the area under the curve represents the total amount of H<sub>2</sub> consumption, while the peaks on the H<sub>2</sub>-TPR profile indicated the reducibility of the catalyst. Together with the pattern of 15% WO<sub>3</sub>/SBA-15, which almost had no hydrogen consumption before 500 °C, it can be inferred that part of WO<sub>3</sub> may be reduced at lower temperatures. This opposite trend in reduction behavior implied that there was a possible electronic interaction between NiO and WO<sub>3</sub>. These results were in line with XRD and Raman results that there were WO<sub>2</sub> crystallite peaks in reduced Ni–WO<sub>3</sub>/SBA-15 samples and the NiO was embedded in the crystal lattice of WO<sub>3</sub>.

In order to further explore the reduction behavior of the Ni–WO<sub>3</sub>/SBA-15 catalyst, the H<sub>2</sub>-TPR results of 3%Ni–15%WO<sub>3</sub>/SBA-15 with different pretreatment conditions were discussed. Fig. 4b gives the H<sub>2</sub>-TPR curves of catalysts pretreated at different temperatures. It can be found that the hydrogen consumption decreased with the pretreated temperature, revealing that the higher the reduction temperature was used, the more metallic oxides were reduced. Fig. 4c, the effect of pretreated time on TPR curves of the catalyst, also displayed the same trend as Fig. 4b. Concerning the decreased hydrogen consumption with the increase in pretreatment temperature or time, it is believed due to the following reason. At first, metallic oxides on the surface were reduced, and further reduction was delayed for the underlayers of catalysts until much higher temperature or longer time was used. Based on above description, it can be concluded that the WO<sub>3-x</sub> may be formed after the catalyst being treated at 500 °C for 1 h in a H<sub>2</sub> atmosphere. Interestingly, the H<sub>2</sub> desorption peak appeared at about 275 °C implied that H<sub>2</sub> was adsorbed strongly by reduced metallic Ni species on the catalyst surface. It can promote the breakage of H–H bond of H<sub>2</sub> molecule and produce active hydrogen atom. These atoms spill over on the WO<sub>3</sub> and migrate away from the Ni site, which is helpful to the formation of H<sub>3</sub>O<sup>+</sup> and the hydrogenation of unsaturated intermediates during reaction process [21,22].

To make an intensive study of the interaction between NiO and WO<sub>3</sub> of the catalyst, XPS analysis was conducted. Fig. 5 shows the XPS spectra of Ni2p and W4f of different catalysts. In comparison with the binding energy of Ni2p<sub>3/2</sub> of 3%Ni/SBA-15 catalyst (855.1 eV), that of Ni2p<sub>3/2</sub> in the 3%Ni–15%WO<sub>3</sub>/SBA-15 catalyst (856.7 eV) positively shifted about 1.6 eV. This result implied a possible electronic interaction occurring between these two oxides. Specifically, the nickel of NiO donated partial electrons to the tungsten of WO<sub>3</sub>, making the nickel electron-deficient and the tungsten electron-enriched. The above conclusion is consistent with the results of H<sub>2</sub>-TPR that compared with Ni/SBA-15 and WO<sub>3</sub>/SBA-15, the reducibility of NiO in the Ni–WO<sub>3</sub>/SBA-15 catalysts lowered, while that of WO<sub>3</sub> enhanced. The electron-deficient Ni active sites

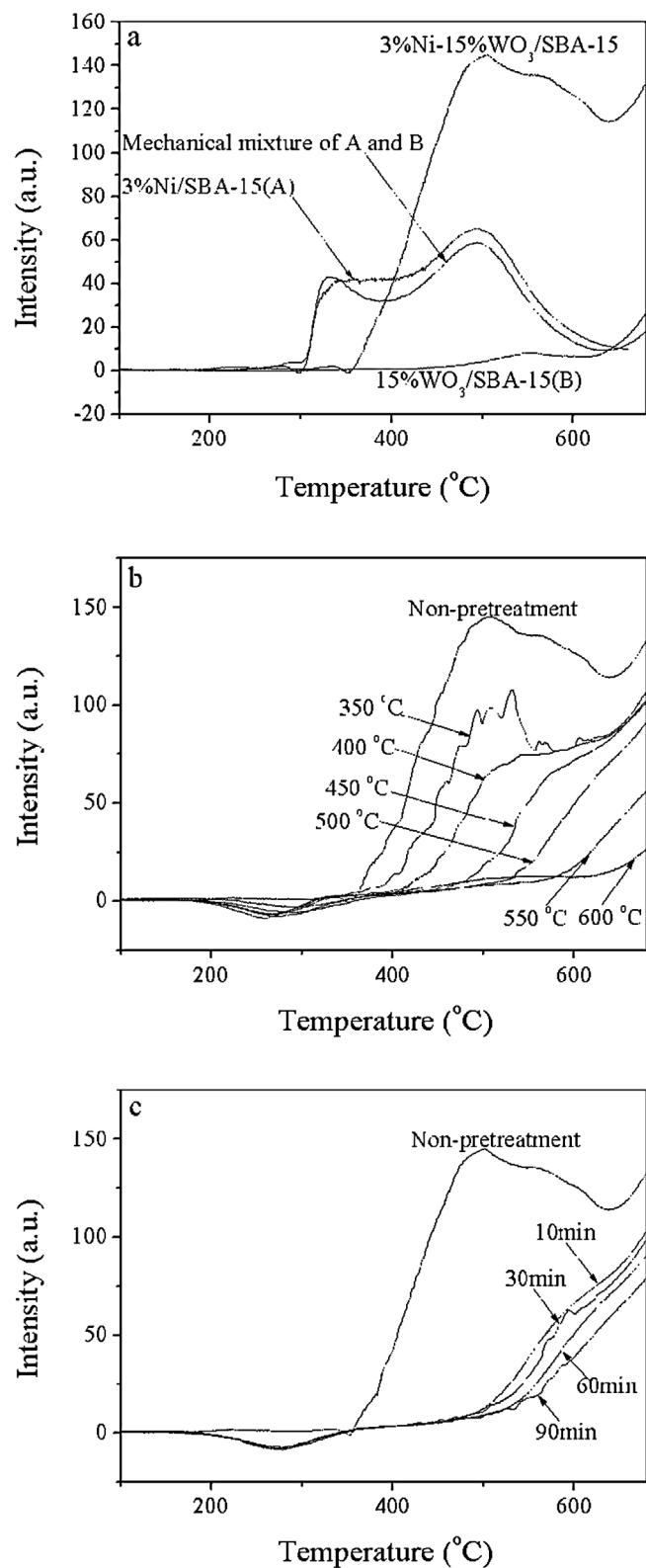


Fig. 4. H<sub>2</sub>-TPR patterns of various samples. (a) 3%Ni/SBA-15(A), 15%WO<sub>3</sub>/SBA-15(B), mechanical mixture of A and B, and 3%Ni–15%WO<sub>3</sub>/SBA-15. (b) 3%Ni–15%WO<sub>3</sub>/SBA-15 pretreated with different reduction temperature. (c) 3%Ni–15%WO<sub>3</sub>/SBA-15 pretreated with different reduction time.

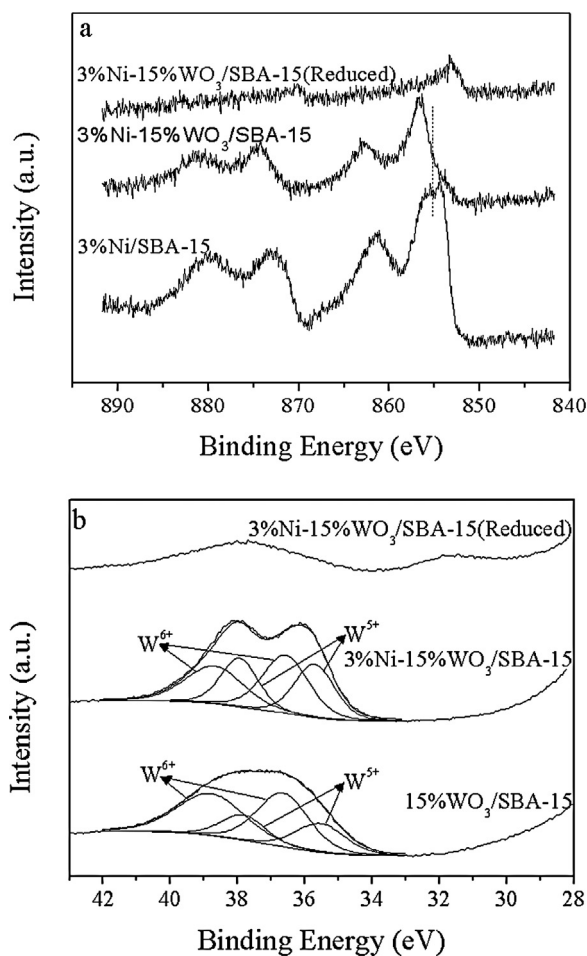


Fig. 5. XPS spectra of different catalysts. (a) Ni2p3/2 and (b) W4f.

also can explain why 3%Ni–15%WO<sub>3</sub>/SBA-15 catalysts had higher hydrogenation activity than that of 3%Ni/SBA-15 catalysts. This is in line with previous report that the hydrogen dissociative chemisorption on the electron-deficient Ni centers is more favorable than that on the electron-enriched ones [23]. However, the change of binding energy of W4f was not manifest. This might be due to the following factors. On the one hand, the WO<sub>3</sub> loading is five times than nickel. On the other hand, the atomic weight of tungsten is several times more than that of nickel. Thus, the change of the binding energy of tungsten was not as sensitive as that of nickel.

More importantly, the XPS can be used to confirm the valance state of nickel and tungsten oxides. As shown in Fig. 5b, the W4f doublets at 38.8 and 36.7 eV were attributed to W<sup>6+</sup> atoms, and the lower ones at 37.8 and 35.6 eV corresponded to W<sup>5+</sup> atoms [24]. In this case, additional electrons are proposed to result from oxygen vacancies which are formed during the synthetic process as precedent report [24]. After the induction of NiO, the area ratio of W<sup>5+</sup> atoms to W<sup>6+</sup> atoms increased, which indicated that more W atoms with low valence state generated due to the intercalation of NiO into the WO<sub>3</sub> crystalline structure resulting in more oxygen vacancies. It is worth to noting that after hydrogen reduction, the peak of high valence of W was weakened, and a much weak peak appeared at 31.5 eV, indicating that more tungsten oxide of high valence state was reduced and W<sup>4+</sup> might be formed in the reduced sample [25]. This result was in line with the XRD result. Although the reduced 3%Ni–15%WO<sub>3</sub>/SBA-15 sample was not protected by the inert atmosphere, it might not be oxidized before the XPS analysis. It is well known that the oxidization of metal Ni is easier than WO<sub>3-x</sub>. But from Fig. 5a, one still can see that metal

**Table 1**  
Effect of WO<sub>3</sub> loading on conversion of cellulose.<sup>a,b</sup>

WO <sub>3</sub> loading (%)	Conversion (%)	Yield (%)				
		EG	1,2-PG	1,2-BG	1,2-HG	Glycerol
5	100	14.6	8.1	2.2	Trace	6.8
10	100	29.2	7.9	1.9	Trace	6.9
15	100	40.3	8.9	2.6	Trace	8.8
20	100	40.9	6.6	2.1	Trace	3.3

<sup>a</sup> Reaction conditions: cellulose 1.0 g, catalyst 0.25 g, deionized water 40 g, temperature 230 °C, initial H<sub>2</sub> pressure 6 MPa, time 6 h.

<sup>b</sup> EG—ethylene glycol; 1,2-PG—1,2-propylene glycol; 1,2-BG—1,2-butanediol; 1,2-HG—1,2-hexanediol.

Ni may exist in the sample because there was a peak at 853.6 eV, which could be assigned to the metal Ni. On the other hand, it is known that at room temperature, the oxidation of WO<sub>x</sub> (X < 3) is comparatively slow [26]. It is thus suggested that the XPS results of reduced sample without inert atmosphere protection might be used to reflect the real state of sample surface. As discussion above, it can be further confirmed that WO<sub>3-x</sub> was formed after catalysts pretreated with hydrogen.

### 3.2. Effect of different WO<sub>3</sub> loading

In this reaction system, there are two crucial steps to transform cellulose into EG: the C–C bond cleavage on active sites of tungsten oxide species and hydrogenation of intermediates on hydrogenation active sites of Ni. Firstly, the effect of WO<sub>3</sub> loading on the catalytic conversion of cellulose over Ni–WO<sub>3</sub>/SBA-15 was evaluated. And the experimental results were summarized in Table 1. For the WO<sub>3</sub>-free catalyst (as shown in Table S1), the primary product was hexitol with a yield of 13.7%, and only 6.0% EG yield was obtained. In contrast, with the introduction of WO<sub>3</sub>, even in a minor amount (5%), the EG yield was elevated greatly, up to 14.6%. Moreover, the EG selectivity increased with the rise of WO<sub>3</sub> loading, reaching maximum (40.3%) when the WO<sub>3</sub> loading 15%WO<sub>3</sub> was loaded. But further increasing the WO<sub>3</sub> loading to 20%, the EG selectivity almost remained unchanged. This implied that 15% WO<sub>3</sub> loading was enough for cellulose conversion and higher loading was unnecessary. Compared with previous report that a good EG selectivity can be obtained over a supported catalyst with 50% WO<sub>3</sub> loading, an excellent selectivity to EG was obtained over Ni–WO<sub>3</sub>/SBA-15 catalyst at much lower WO<sub>3</sub> loading in this catalytic system [16]. It provided evidence that this synergy between Ni and WO<sub>3</sub> was beneficial to the EG formation.

Supplementary material related to this article can be found, in the online version, at <http://dx.doi.org/10.1016/j.molcata.2013.10.002>.

Considering the performance and cost of the catalyst, 15%WO<sub>3</sub> loading was fixed for further studies.

### 3.3. Effect of different Ni loading

It is generally known that the high Ni loading is beneficial to boost hydrogenation, but more importantly, it may cover part of active sites of tungsten oxide species [27,28]. Therefore, to achieve a high EG selectivity, the optimization of the ratio of metal Ni to WO<sub>3</sub> proves to be very important. Related experiment results were summarized in Table 3.

As shown in Table 2, the EG yield increased with the rise of Ni loading, and reached the highest (70.7%) at 3% loading. However, further increasing in Ni loading to exceed 5% led to a slight decline in the yield toward EG, the EG yield over catalysts with 5%, 10%, 15% and 20% Ni loading were 51.12%, 53.64%, 40.31%, 30.43%, respectively. This may be caused by two reasons. One is that the higher Ni loading generated more hydrogenolysis active sites,

**Table 2**  
Effect of Ni loading on conversion of cellulose.<sup>a,b</sup>

Ni loading (%)	Conversion (%)	Yield (%)				
		EG	1,2-PG	1,2-BG	1,2-HG	Glycerol
1	100	28.3	2.7	3.3	Trace	Trace
3	100	70.7	5.9	4.2	0.5	0.3
5	100	51.1	5.4	2.6	Trace	Trace
10	100	53.6	8.5	3.5	Trace	3.7
15	100	40.3	8.9	2.6	Trace	8.8
20	100	30.3	6.3	1.4	Trace	5.9

<sup>a</sup> Reaction conditions: cellulose 1.0 g, catalyst 0.25 g, deionized water 40 g, temperature 230 °C, initial H<sub>2</sub> pressure 6 MPa, time 6 h

<sup>b</sup> EG—ethylene glycol; 1,2-PG—1,2-propylene glycol; 1,2-BG—1,2-butanediol; 1,2-HG—1,2-hexanediol.

which competed with WO<sub>3</sub> and led to the non-selective cleavage of C—C bond. The other one is that excessive Ni covered part active sites of tungsten oxide species. All of these would result in the formation of more cracking products such as monoalcohols, carbon monoxide, and carbon dioxide

Noticeably, for the 3% Ni/SBA-15 (as shown in Table S1), its hydrogenation activity was insufficient due to the fact that the pH value of reaction solution was 3.5. However, the value was about 7.0 over 3%Ni-15WO<sub>3</sub>/SBA-15 catalyst. It also proved that the introduction of tungsten oxides enhanced the hydrogenation ability of Ni. Together with the fact that only trace products were acquired over mechanical mixed 3% Ni/SBA-15 and 15%WO<sub>3</sub>/SBA-15 catalyst (as shown in Table S1), it further indicated that the synergy between Ni and tungsten oxides was the key to obtain the high EG selectivity.

#### 3.4. Effect of reduction temperature of catalysts

H<sub>2</sub>-TPR results had proved that reduction temperature had great effect on Ni and W oxide state, especially on the reduction of tungsten oxide. So, the impact of catalysts reduction temperature on cellulose conversion was examined. As shown in Table 3, the selectivity of EG was nearly zero when the catalyst was reduced at 350 °C. Together with the result of H<sub>2</sub>-TPR that only nickel oxide could be reduced at 350 °C, it could be confirmed that both metal Ni and WO<sub>3</sub> were not responsible for the high EG selectivity. These results also can explain previous researchers' experimental results that only the 50% WO<sub>3</sub> loading can obtain a good EG selectivity [16]. This may result from that high WO<sub>3</sub> loading may have the enough WO<sub>3</sub> locating on the surface of support and they can be partly reduced under those reaction conditions [29]. The yield of EG increased remarkably with the reduction temperature, and reached the maximum at 500 °C and then decreased. This was coincident with the H<sub>2</sub>-TPR results that more WO<sub>3-x</sub> could be generated at higher temperatures. As to the decrease of EG yield at higher

**Table 3**  
Effect of catalysts reduction temperature on conversion of cellulose.<sup>a,b</sup>

Reduction temperature (°C)	Conversion (%)	Yield (%)				
		EG	1,2-PG	1,2-BG	1,2-HG	Glycerol
350	96.1	Trace	Trace	Trace	Trace	Trace
400	100	26.3	Trace	Trace	Trace	Trace
450	100	57.8	2.5	1.8	0.5	Trace
500	100	70.7	5.9	4.2	0.5	0.3
550	100	64.7	4.6	2.7	0.5	Trace
600	100	58.6	3.8	2.2	0.7	Trace

<sup>a</sup> Reaction conditions: cellulose 1.0 g, catalyst 0.25 g, deionized water 40 g, temperature 230 °C, initial H<sub>2</sub> pressure 6 MPa, time 6 h.

<sup>b</sup> EG—ethylene glycol; 1,2-PG—1,2-propylene glycol; 1,2-BG—1,2-butanediol; 1,2-HG—1,2-hexanediol.

**Table 4**  
Effect of catalysts reduction time on conversion of cellulose.<sup>a,b</sup>

Reduction time (min)	Conversion (%)	Yield (%)				
		EG	1,2-PG	1,2-BG	1,2-HG	Glycerol
10	100	41.9	1.3	0.6	Trace	Trace
30	100	61.8	3.5	2.0	Trace	Trace
60	100	70.7	5.9	4.2	0.5	0.3
90	100	61.1	6.0	3.1	0.5	0.3

<sup>a</sup> Reaction conditions: cellulose 1.0 g, catalyst 0.25 g, deionized water 40 g, temperature 230 °C, initial H<sub>2</sub> pressure 6 MPa, time 6 h

<sup>b</sup> EG—ethylene glycol; 1,2-PG—1,2-propylene glycol; 1,2-BG—1,2-butanediol; 1,2-HG—1,2-hexanediol.

reduction temperatures, it may be ascribed to the sintering of active Ni species, which is in agreement with previous report [30].

#### 3.5. Effect of reduction time of catalysts

To further clarify that WO<sub>3-x</sub> was the active phase for the selective cleavage of C—C bond in the sugar intermediates, the effect of catalysts reduction time on conversion of cellulose was performed. As shown in Table 4, EG selectivity improved dramatically from 41.9% (10 min) to 70.7% (60 min) and then slightly declined with further elongated time. It could be concluded that short reducing time was insufficient to produce enough active sites for cellulose conversion, but the too long reduction time might lead to the sintering of active Ni species and weakened the hydrogenation activity of the catalyst.

#### 3.6. Reaction mechanism

According to the previous research work, we have known that various tungsten compounds have the unique ability for the catalytic conversion of cellulose to EG, especially when they are combined with the hydrogenation component such as Ni and Ru [12–17]. But the genuinely catalytically active species in the selectivity C—C cleavage of cellulose is unknown. To address this issue, some researchers [16] studied the phase change of different tungsten species, such as W, W<sub>2</sub>C, WO<sub>3</sub> and WO<sub>2</sub>, before and after the reaction by surface-sensitive XPS and Raman spectroscopy. It was found that WO<sub>3</sub> always became the main component on the surface of the used catalyst no matter what the tungsten species is initially used. Accordingly, the authors suggested WO<sub>3</sub> should be responsible for the selective cleavage of C—C bond of sugar intermediates. However, under those reaction conditions such as high temperature and high hydrogen pressure, together with the intermediates with aldehyde group and/or hydroxyl, the WO<sub>3</sub> may be partly reduced and it can be slowly oxidized in air. It is well known that some aldehydes and alcohols could reduce some metallic oxides [29]. Therefore, these studies cannot reflect the real state of tungsten species since the oxidation of catalysts might have happened before these characterizations were conducted. Later, Tai et al. [17] found the tungsten oxide recovered immediately after the reaction showed typical XRD pattern of tungsten bronze (H<sub>x</sub>WO<sub>3</sub>) instead of WO<sub>3</sub>, while the H<sub>x</sub>WO<sub>3</sub> was not stable upon exposure to atmosphere and gradually transformed into WO<sub>3</sub>. Therefore, they concluded that the dissolved H<sub>x</sub>WO<sub>3</sub>, transformed through various tungsten species by H<sub>2</sub> under the reaction conditions, was the genuinely catalytically active species for C—C cleavage. Although the non-hexavalent tungsten species are very attractive to be the active species, the dissolved tungsten species may not be very convincing since the tungsten oxide recovered immediately after the reaction must contain some water which will disturb the analysis result. Actually, on the basis of our research results, we proposed that the

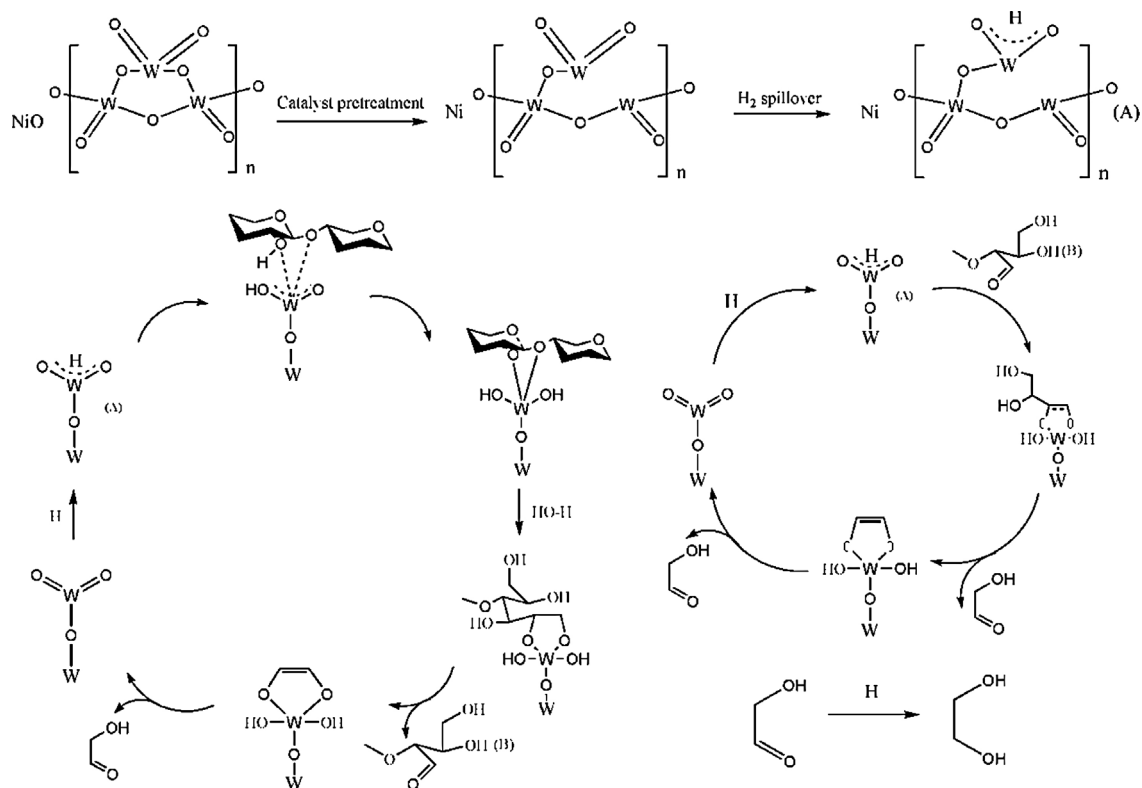


Fig. 6. Proposed mechanism for conversion of cellulose into EG over Ni-WO<sub>3</sub>/SBA-15 catalyst.

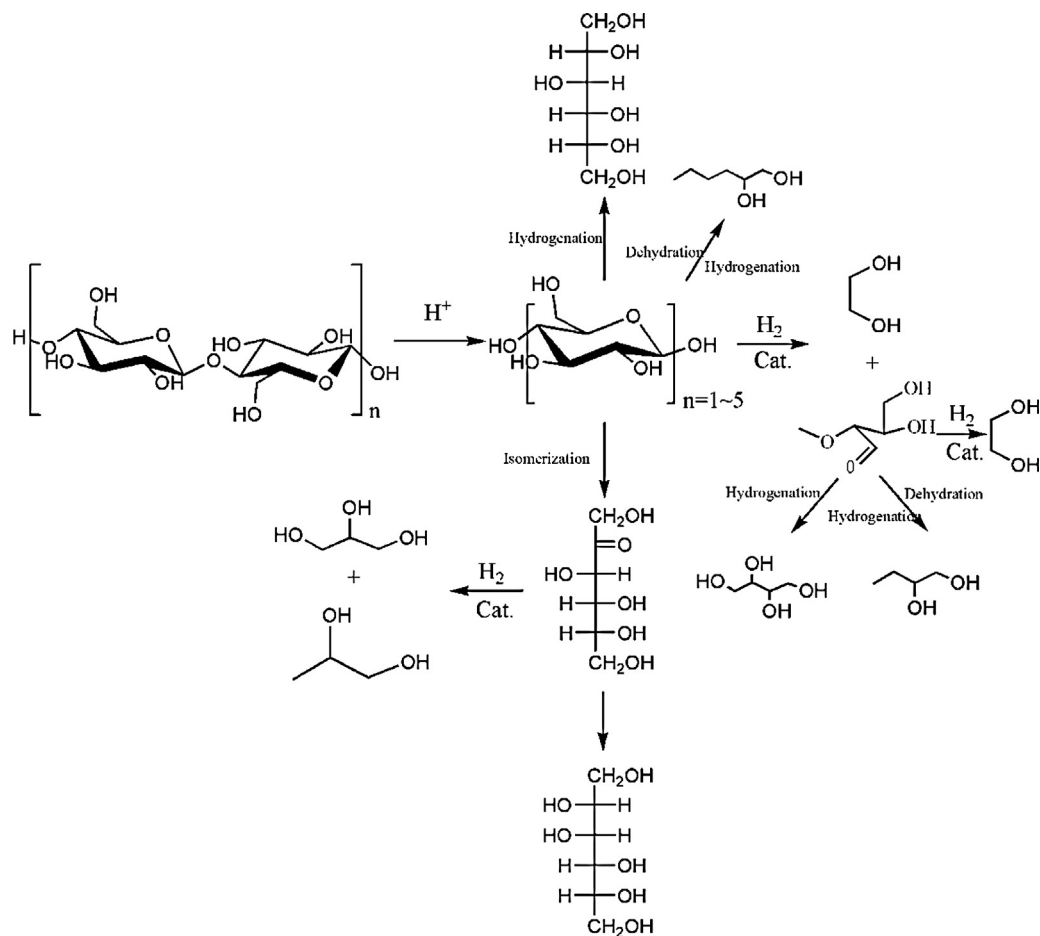


Fig. 7. Proposed reaction pathways involved in hydrolytic hydrogenation of cellulose over Ni-WO<sub>3</sub>/SBA-15.

WO<sub>3-x</sub>, partly reduced WO<sub>3</sub>, was the genuinely active species of tungsten-based catalysts.

For the reaction mechanism of aldoses conversion to polyols, previous research reported that the C–C cleavage of cellulose or sugars follows the retro-aldol pathway [31]. Recently, Zahng and co-workers [17,32] proposed a reaction path way involved the production of EG from cellulose. Firstly, cellulose was hydrolyzed to cellooligosaccharides. Then, cellooligosaccharides were gradually converted into glycolaldehyde through retro-aldol reaction with the assistance of dissolved H<sub>x</sub>WO<sub>3</sub> since glycolaldehyde was always the main product from cellulose conversion over different tungsten-based catalysts without the presence of hydrogenation component. Finally, the intermediate glycolaldehyde was instantly hydrogenated to EG over the hydrogenation catalysts. However, Liu et al. [16] have their own opinion concerning the reaction mechanism because they found the reactions of 2-deoxy-glucose and 2-deoxy-ribose on WO<sub>3</sub> and Ru/C did not follow the retro-aldol mechanism. Therefore, they proposed that cleavage of the C–C bond in the cellulose reaction may proceed through complexation of the sugar intermediates with WO<sub>3</sub>. Specifically, the WO<sub>3</sub> coordinated with the carbonyl oxygen atoms and three hydroxylic oxygen atoms at the α-, β-, and γ-OH groups of the sugars, and then the complexation occurred the rearrangement of the C–C bonds of the sugars. Hayes et al. [33] have previously proposed similar complexation mechanism for the epimerization of aldoses on molybdates.

Based on above discussion and our experimental results, a systematic mechanism for the reaction was proposed, as shown in Fig. 6. We believed that one complexation of the sugar intermediates with HWO<sub>x</sub> might involve in this reaction system. Specifically, there are four stages involved in this process.

Initially, the catalyst pretreatment process leads to the formation of oxygen vacancies via water production. This may produce one drive to adsorb the oxygen of sugar intermediates. Then the intermediate (A) is created via H<sub>2</sub> splitting and spillover from Ni. In the second stage, the intermediate (A) absorbs cellooligosaccharides and/or glucose. Afterwards, the tungsten atoms coordinate with oxygen of 1, 4-glycosidic bond and α-OH, and then hydrogen shifts to oxygen of W=O to produce W–OH. After that, through the rearrangement of the C–C bond and C–O bond produces glycolaldehyde and another reactive intermediate (B) with assistance of a molecule of H<sub>2</sub>O. At the same time, the WO<sub>3-x</sub> is recovered, and receiving the hydrogen by H<sub>2</sub> splitting on nearby Ni sites. The intermediates (B) are transformed into two molecules of glycolaldehyde through the similar coordination and rearrangement processes described above and all glycolaldehydes are quickly hydrogenated to EG on the Ni site. These steps together constitute the whole cyclic process. Additionally, the possible reaction routes involved in cellulose hydrogenolysis was proposed in Fig. 7.

#### 4. Conclusion

Ni–WO<sub>3</sub>/SBA-15 catalysts were synthesized and evaluated for the catalytic conversion cellulose into polyols, especially EG. The

best result was obtained on 3% Ni–15%WO<sub>3</sub>/SBA-15 which exhibited complete conversion of cellulose with up to 70.7% EG yield. By detailed characterization of Ni–WO<sub>3</sub>/SBA-15 using several physicochemical methods, it was found that there was a strong electronic interaction between nickel oxide and tungsten trioxide, and that WO<sub>3-x</sub> was formed on SBA-15 after H<sub>2</sub>-reduction of NiO–WO<sub>3</sub>/SBA-15 at 500 °C. Additionally, a possible catalytic reaction mechanism for the transformation of cellulose into EG over Ni–WO<sub>3</sub>/SBA-15 was proposed.

#### Acknowledgement

This work was financially supported by the Major State Basic Research Development Program of China (973 Program) (No. 2012CB215305).

#### References

- [1] Y. Sun, J. Cheng, *Bioresour. Technol.* 83 (2002) 1–11.
- [2] N. Mosier, C. Wyman, B. Dale, R. Elander, Y.Y. Lee, M. Holtzapfle, M. Ladisch, *Bioresour. Technol.* 96 (2005) 673–686.
- [3] A. Fukuoka, P.A. Dhepe, *Angew. Chem. Int. Ed.* 45 (2006) 5161–5163.
- [4] C. Luo, S. Wang, H. Liu, *Angew. Chem. Int. Ed.* 46 (2007) 7636–7639.
- [5] W. Deng, X. Tan, W. Fang, Q. Zhang, Y. Wang, *Catal. Lett.* 133 (2009) 167–174.
- [6] S. Van de Vyver, J. Geboers, M. Dusselier, H. Schepers, T. Vosch, L. Zhang, G. Van Tendeloo, P. Jacobs, S. Bert, *ChemSusChem* 3 (2010) 698–701.
- [7] L.N. Ding, A.Q. Wang, M.Y. Zheng, T. Zhang, *ChemSusChem* 3 (2010) 818–821.
- [8] J. Geboers, S. Van de Vyver, K. Carpentier, K. de Blochouse, P. Jacobs, B. Sels, *Chem. Commun.* 46 (2010) 3577–3579.
- [9] R. Palkovits, K. Tajvidi, A.M. Ruppert, J. Procelewska, *Chem. Commun.* 47 (2011) 576–578.
- [10] R. Palkovits, K. Tajvidi, J. Procelewska, R. Rinaldi, A. Ruppert, *Green Chem.* 12 (2010) 972–978.
- [11] J. Geboers, S. Van de Vyver, K. Carpentier, P. Jacobs, B. Sels, *Catal. Commun.* 47 (2011) 5590–5592.
- [12] N. Ji, T. Zhang, M. Zheng, A. Wang, H. Wang, X. Wang, J.G. Chen, *Angew. Chem.* 120 (2008) 8638–8641.
- [13] M. Zheng, A. Wang, N. Ji, J. Pang, X. Wang, T. Zhang, *ChemSusChem* 3 (2010) 63–66.
- [14] Y. Zhang, A. Wang, T. Zhang, *Chem. Commun.* 46 (2010) 862–864.
- [15] I.G. Baek, S.J. You, E.D. Park, *Bioresour. Technol.* 114 (2012) 684–690.
- [16] Y. Liu, C. Luo, H. Liu, *Angew. Chem.* 124 (2012) 3303–3307.
- [17] Z. Tai, J. Zhang, A. Wang, M. Zheng, T. Zhang, *Chem. Commun.* 48 (2012) 7052–7054.
- [18] C.V. Ramana, S. Utsunomiya, C.M. Julien, U. Becker, *ECS Trans.* 1 (2006) 37–42.
- [19] T. Kubo, Y. Nishikitani, *J. Electrochem. Soc.* 145 (1998) 1729–1733.
- [20] C. Martin, P. Malet, G. Solana, V.J. Rives, *Phys. Chem. B* 102 (1998) 2759–2768.
- [21] R. Prins, *Chem. Rev.* 112 (2012) 2714–2738.
- [22] A. Shrotri, A. Tanksale, J.N. Beltramini, H. Gurav, S.V. Chilukuri, *Catal. Sci. Technol.* 2 (2012) 1852–1858.
- [23] S. Yoshida, H. Yamashita, T. Funabiki, T. Yonezawa, *J. Chem. Soc., Faraday Trans.* 1 80 (1984) 1435–1446.
- [24] Yang, R. Gao, W.-L. Dai, K. Fan, *J. Phys. Chem. C* 112 (2008) 3819–3826.
- [25] D.D. Sarma, C.N.R. Rao, *J. Electron Spectrosc. Relat. Phenom.* 20 (1980) 25–45.
- [26] G. Leftheriotis, S. Papaefthimiou, P. Yianoulis, A. Siokou, *Thin Solid Films* 384 (2001) 298–306.
- [27] R.A. Dalla Betta, A.G. Piken, M. Shelef, *J. Catal.* 40 (1975) 176–183.
- [28] Y. Okamoto, Y. Nitta, T. Imanaka, S. Teranishi, *J. Catal.* 64 (1980) 397–404.
- [29] P.-Y. Silvert, R. Herrera-Urbina, K. Tekaiia-Elhissen, *J. Mater. Chem.* 7 (1997) 293–299.
- [30] J. Sehested, *J. Catal.* 217 (2003) 417–426.
- [31] K.Y. Wang, M.C. Hawley, T.D. Furney, *Ind. Eng. Chem. Res.* 34 (1995) 3766–3770.
- [32] A. Wang, T. Zhang, *Acc. Chem. Res.* 46 (2013) 1377–1386.
- [33] M.L. Hayes, N.J. Pennings, A.S. Serianni, R. Barker, *J. Am. Chem. Soc.* 104 (1982) 6764–6769.